Cross Technology Interference Mitigation in Body Area Networks: an Optimization Approach

Jocelyne Elias , Stefano Paris and Marwan Krunz

***Abstract*—In recent years, wearable devices and Wireless Body Area Networks have gained momentum as a means to monitor people's behavior and simplify their interaction with the surrounding environment, thus representing a key element of the Body-to-Body Networking (BBN) paradigm. Within such paradigm, several transmission technologies like 802.11 and 802.15.4 that share the same unlicensed band (namely the ISM band) coexist, increasing dramatically the level of interference and, in turn, negatively affecting network performance. In this paper, we analyze the Cross Technology Interference (CTI) caused by the utilization of different transmission technologies that share the same radio spectrum. We formulate an optimization model that considers internal interference as well as CTI in order to mitigate the overall level of interference within the system, taking explicitly into account node mobility. We further develop three heuristic approaches to efficiently solve the interference mitigation problem in large-scale network scenarios. Finally, we propose a protocol to compute the solution that minimizes CTI in a distributed fashion. Numerical results show that the proposed heuristics represent efficient and practical alternatives to the optimal solution for solving the CTI mitigation problem in large scale BBN scenarios.**

Index Terms*—Body-to-Body Networks, Cross Technology Interference, Interference Mitigation, Optimization.

I. Introduction

The ongoing evolution of wireless technologies has fostered the development of innovative network paradigms like Wireless Body Area Networks (WBANs), where the pervasive deployment of wireless devices endowed with sensing capabilities interweaves the physical and digital worlds, thus enabling the development of enhanced services. Wireless Body Area Networks, and more specifically Body-to-Body Networks (BBNs), are emerging solutions for the monitoring of people's behavior and their interaction with the surrounding environment. In its most common configuration, a BBN consists of several WBANs, as illustrated in Figure 1. Each WBAN is composed of wearable sensor nodes, connected through the 802.15.4 protocol (i.e., ZigBee) to their mobile terminal. The set of wearable sensors may be used to consistently monitor people's vital signs, like blood pressure, heart rate, skin temperature, or important environmental parameters like temperature and humidity. Furthermore, wireless headsets can be used to enable communications among BBN users, while glasses like those recently proposed by Google and Microsoft can be connected wirelessly with a smartphone to provide augmented reality [1].

Mobile terminals are usually equipped with two radio interfaces, implementing the 802.15.4 and the 802.11 protocols. These protocols are used, respectively, for coordinating the activity of wearable sensor nodes and to form the wireless backhaul infrastructure among the WBANs of the BBN. Due to the broadcast nature of the wireless medium and the limited radio spectrum, data transmissions between the devices involved in BBN communications may interfere, thus reducing the network performance of the entire system. More specifically, successful data transmissions over two or more conflicting wireless links that use the same PHY technology cannot be simultaneously performed. Furthermore, as illustrated in [2], the cross-technology interference (CTI) caused by frequency overlap across different wireless technologies like ZigBee and WiFi can highly affect the performance of WBANs both in terms of achievable throughput and reliability. In particular, data transmissions within ZigBee networks can be completely prevented by WiFi communications, which use 10 to 100 times higher transmission powers.

On the other hand, given the scarce availability of the radio spectrum, many existing wireless technologies are forced to use the same unlicensed frequency bands. For example, IEEE 802.11 (WiFi), IEEE 802.15.1 (Bluetooth) and IEEE 802.15.4 (ZigBee) all share the same 2.4 GHz ISM band. Hence, interference across these technologies can lead to loss of reliability and inefficient use of the radio spectrum. While authors in [3], [4] have recently proposed to use ultrasonic waves and light to wirelessly interconnect in/on-body devices, RF systems still represent the de-facto standard for interconnecting off-the shelf wearable devices [1].

Our main contributions are as follows:

- We analyze the problem of mutual and cross-technology interference in a dynamic BBN system, where mobile devices use simultaneously different access technologies over the same frequency spectrum.
- We formulate the interference mitigation as an optimization problem and an interference graph to model cross-technology transmission conflicts. We explicitly consider network dynamics due to nodes mobility by optimizing the worst interference caused by nodes proximity. Furthermore, we show that the problem is NP-hard.
- We present three heuristic solutions, namely a customized randomized rounding approach, a tabu-search scheme, and a sequential fixing algorithm, to efficiently solve the problem even for large-scale network scenarios. Throughout our algorithmic design, we assume a common view of the network topology and its dynamics.
- We describe a signaling protocol to disseminate and update the topology information in order to converge to a common view of the network topology and implement

Jocelyne Elias and Stefano Paris are with LIPADE, Université Paris Descartes. Marwan Krunz is with the ECE Department, University of Arizona.

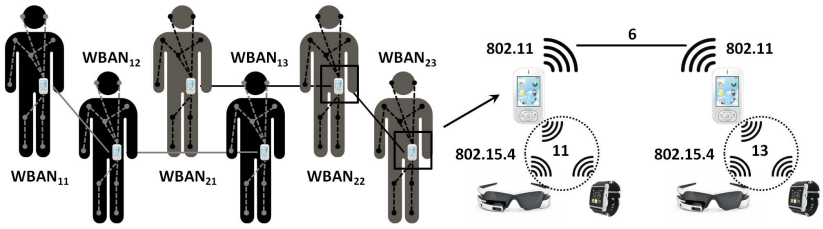

Fig. 1: Network scenario: Two BBNs corresponding to two different groups of people (i.e., black and gray) are using the same set of unlicensed channels.

our CTI mitigation algorithms in a fully distributed fashion.

- We perform thorough numerical evaluation of the proposed mechanisms, considering both static and mobile network scenarios. Specifically, we calculate the achievable throughput of the system using a TDMA approach to coordinate the access of BBN transmissions.

Numerical results show that the proposed model and heuristics significantly reduce the level of interference between different technologies within a BBN scenario, thus improving the overall network performance relative to the standard Adaptive Frequency Hopping (AFH) scheme.

The paper is structured as follows. Section II discusses related work. Section III introduces the communication model as well as the assumptions considered in our work. Section IV formulates the interference mitigation problem as an optimization model, while Section V describes the heuristic approaches designed to efficiently solve this problem. Section VI presents a distributed protocol to minimize CTI. Section VII illustrates and analyzes numerical results that show the efficiency and validity of our approaches. Finally, concluding remarks are discussed in Section VIII.

II. Related Work

In this section, we discuss the most relevant works that deal with the problem of interference mitigation between different technologies (i.e., ZigBee and WiFi) operating over the same frequency spectrum. The problem of minimizing 802.11 interference on ZigBee medical sensors was addressed in [5], where the authors proposed a solution that utilizes hardware consisting of both 802.15.4 and 802.11 transmitters. The goal is to temporarily block out 802.11 messages for a time window large enough such that ZigBee devices can successfully transmit their messages. To do so, the authors developed two types of solutions: (i) periodically jam 802.11 to fit ZigBee messages into empty time frames, and (ii) transmit a CTS message directly before a ZigBee message.

Instead of trying to avoid interference from 802.11 traffic, the authors in [2] focused on improving the coexistence of 802.15.4 and 802.11 devices that operate in overlapping frequency channels. More specifically, they presented a MAC layer solution (called BuzzBuzz) that enables 802.15.4 nodes to coexist with WiFi networks by using multi-headers and forward error correction codes to overcome the packet loss caused by 802.11 interference. A ZigBee frame control protocol (WISE) was proposed in [6] to deal with the interference between ZigBee and WiFi, demonstrating solid performance gains (19.5% and 42.5%) over B-MAC (the default MAC protocol in TinyOS) and OppTx [7], [8], respectively. WISE first predicts the length of white space in WiFi traffic based on a Pareto model and then adapts the frame size to maximize the throughput efficiency. In [9], [10] the authors proposed two mechanisms that enable reliable coexistence of ZigBee and WiFi networks. The first mechanism includes a frequency flip scheme and a cooperative carrier signaling that prevent mutual interference between cooperative ZigBee nodes. In contrast, the second scheme presents a busy tone scheduler that minimizes the interference due to WiFi networks.

A tool for understanding 802.11 performance in heterogeneous environments without the use of dedicated infrastructures was presented in [11]. This tool, called WiMed, uses 802.11 NICs to produce a time allocation map, showing how the medium is used. It can detect non-802.11 sources of interference using NIC registers and bit-error analysis.

In [12], the authors considered a 802.11-based multiradio mesh network with stationary wireless routers. They addressed the problem of assigning channels to communication links, while minimizing the overall mutual interference among wireless links that use the same technology. A random coloring scheme is proposed in [13] both to reduce mutual interference of nearby WBANs and achieve high spatial reuse, whereas the work [14] presents a transmission scheduling scheme to maximize resource utilization under SINR constraints. In contrast, we consider a BBN network, composed of wireless sensors that are equipped with ZigBee interfaces and mobile terminals that are equipped with both ZigBee and WiFi interfaces. Our proposed solutions aim at minimizing both the mutual (i.e., WiFi-WiFi and ZigBee-ZigBee) and the cross-technology (i.e., WiFi-ZigBee) interference, considering a set of consecutive time epochs to represent the mobility of WBANs.

In summary, none of the above reviewed works has investigated an optimization framework to jointly minimize the mutual and cross technology interferences in a mobile BBN scenario composed of several WBANs.

III. Network Model

This section presents the network model and assumptions we adopt in the design of our interference mitigation approach. We consider a BBN system, composed of a set $\mathcal{N}$ of wearable Mobile Terminals (MTs) that use both the 802.15.4 protocol (i.e., ZigBee) [1] to communicate with sensor nodes within a

[1]Since we only consider the physical specifications of IEEE 802.15.4 and ZigBee to model interference, in the paper we interchangeably use these two terms even if they are not exactly the same.

WBAN and the IEEE 802.11 wireless standard (i.e., WiFi) to create a backhaul infrastructure for inter-WBANs' communications, as illustrated in Figure 1. The two sets $\mathcal{K}_w$ and $\mathcal{K}_z$ identify the (potentially overlapping) radio channels defined by the WiFi and ZigBee technologies, respectively. In particular, according to the standards, $\mathcal{K}_w \in [1-11]$ and $\mathcal{K}_z \in [11-26]$.

The operating time of the system is divided into a set $\mathcal{T}$ of consecutive epochs. We assume that during each epoch the network topology does not change. Specifically, let $\mathcal{L}_w(t)$ represent the set of WiFi links established by mobile terminals during epoch $t \in \mathcal{T}$. $\mathcal{L}_w(t)$ may vary between two consecutive epochs due to WBAN mobility. This set contains the triplet (i,j,t) if at time epoch t, nodes i and j can establish a communication link, i.e., $\mathcal{L}_w(t) = \{(i,j,t) : i \in \mathcal{N}, j \in \mathcal{N},$ and $SINR(i,j,t) \geq \sigma_w\}$, namely if the SINR is higher than a threshold σ_w opportunely set according to the WiFi technology. In contrast, the set $\mathcal{L}_z$, which contains the ZigBee links used for intra-WBAN communication, does not change during the entire operating time of the system. Note that $\mathcal{L}_z$ contains only the mobile terminal identifier that represents the worst link established by the mobile terminal with the ZigBee nodes within the WBAN that it coordinates. Indeed, a time-slotted access scheme is used by the mobile terminal to coordinate intra-WBAN communications.

To model the different types of interference caused by different wireless technologies, we propose a *cross-technology* weighted conflict graph for representing pairs of interfering wireless links. Specifically, we introduce the concept of *cross-conflict edges* to model the Cross Technology Interference (CTI). Such an edge connects two vertices that represent two interfering links that use different technologies (i.e., WiFi and ZigBee). Therefore, the weighted conflict graph $G_c(\mathcal{V}_c(t), \mathcal{E}_c(t))$ is defined over the vertex set $\mathcal{V}_c(t) = \mathcal{L}_w(t) \cup \mathcal{L}_z$, which contains all wireless links established by mobile terminals (either WiFi or ZigBee). The set $\mathcal{E}_c(t)$ includes edges that model interfering links of the same radio technology as well as cross-technology edges. For the sake of clarity, we explicitly define the three subsets that compose $\mathcal{E}_c(t)$: $\mathcal{E}_c^w(t)$ and $\mathcal{E}_c^z(t)$ contain respectively edges that model interfering WiFi and ZigBee links, whereas $\mathcal{E}_c^{wz}(t)$ includes cross-technology edges. Since WiFi channels may overlap, the weight of the edge connecting two interfering WiFi links is proportional to the intersection area between the spectrum of the two signals [15].

Conversely, when two vertices in $\mathcal{V}_c(t)$ represent wireless links that operate using different radio technologies, a cross-technology edge is used to indicate that the two links interfere if they use overlapping channels, like, for example, by tuning $e_1 \in \mathcal{L}_w(t)$ on WiFi channel 1 and $e_2 \in \mathcal{L}_z(t)$ on ZigBee channel 12.

Figure 2 shows the cross-technology conflict graph of the network scenario in Figure 1, where solid lines are used to represent the conflict edges that model the interference between links of the same technology, whereas dashed lines correspond to cross-conflict edges. Note that we consider only one ZigBee link for any WBAN in the set $\mathcal{L}_z$. Therefore, the cross-technology conflict graph accounts for four 802.11 and six 802.15.4 vertices to represent, respectively, four WiFi links and six ZigBee WBANs of Figure 1. We observe that mobile terminals can obtain a good estimation of the conflict graph G_c using historical measurements that they can collect during their daily activities. Indeed, transmission conflicts can be reasonably predicted from such measurements, since human mobility patterns are highly repetitive [16].

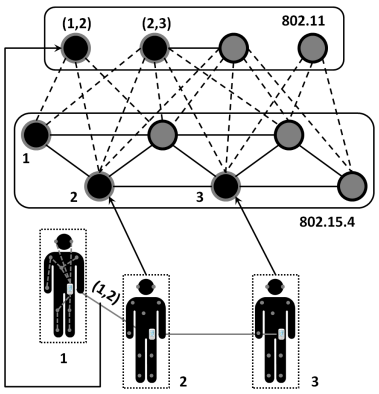

Fig. 2: Cross-technology conflict graph representing interfering wireless links of the scenario illustrated in Figure 1. Small gray dots represent ZigBee sensors.

Formally, we represent the mutual interference caused by using two overlapping WiFi channels by the $|\mathcal{K}_w| \times |\mathcal{K}_w|$ matrix $\boldsymbol{C}$, whose element $c_{kh} \in [0,1]$ has a value that is proportional to the overlapping spectrum of the two signals [15]. Similarly, we model the Cross Technology Interference between two overlapping channels using a $|\mathcal{K}_w| \times |\mathcal{K}_z|$ binary matrix $\boldsymbol{A}$, whose element $a_{kh} = 1$ states that WiFi channel $k \in \mathcal{K}_w$ interferes with ZigBee channel $h \in \mathcal{K}_z$. In contrast, two different ZigBee channels do not interfere between each other, since all channels defined by the IEEE 802.15.4 standard are orthogonal.

The connectivity among the mobile terminals that belong to the same BBN and through which the sensor nodes of different WBANs can communicate, is defined using the $|\mathcal{L}_w| \times |\mathcal{L}_w|$ binary matrix $\boldsymbol{B}$, whose element $b_{uv} = 1$ indicates that WiFi links u and v belong to the same BBN.

Finally, regarding the underlying traffic model, we design our interference mitigation mechanism assuming uniform traffic. However, we emphasize that the proposed model and algorithms can be extended to other traffic models [17].

IV. Optimal Cross-Technology Interference Mitigation (CTIM) Problem

To mitigate the cross-technology interference caused by the utilization of different transmission technologies on the same unlicensed spectrum, we propose to jointly assign 802.11b/g and 802.15.4 frequencies to device interfaces in order to minimize the maximum number of interfering links using overlapping wireless channels. In fact, the minimization of the worst case guarantees a minimum level of service in terms of achievable performance while simplifying the distributed computation of the solution, as we will illustrate in Section VI. In the following, we formalize the Integer Linear Programming (ILP) model for solving the Cross Technology Interference

Mitigation (CTIM) problem. We first introduce the decision variables used in our model and then provide the ILP description of the problem.

Binary variables $\{x^t_{uk} : u \in \mathcal{L}_w(t), k \in \mathcal{K}_w, t \in \mathcal{T}\}$ represent the temporal assignment of WiFi channels to wireless links established among the mobile terminals of a BBN using their WiFi interfaces. Specifically, $x^t_{uk} = 1$ indicates that channel $k \in \mathcal{K}_w$ is assigned to wireless link $u \in \mathcal{L}_w$ throughout epoch $t \in \mathcal{T}$. Similarly, the set of binary variables $\{y^t_{vh} : v \in \mathcal{L}_z, h \in \mathcal{K}_z, t \in \mathcal{T}\}$ represents the ZigBee channels assigned to all communication links used by the wearable sensors of WBAN v. As discussed in the previous section, we consider only one representative link of the WBAN, since we are assuming that all the sensors of a WBAN operate on the same channel.

Let $I^w_{u,v}(t)$ represent the *worst* mutual interference in epoch t caused by data transmissions over two conflicting links u and v that use WiFi protocol. Such interference, $\forall t \in \mathcal{T}, \forall (u,v) \in \mathcal{E}^w_c(t)$, varies as a function of the binary decision variables x^t_{uk} and x^t_{vh} as follows:

$$0 \leq I^w_{u,v}(t) \leq \sup_{k,h \in \mathcal{K}_w} \{c_{kh} \cdot (x^t_{uk} + x^t_{vh} - 1)\} \tag{1}$$

where the right hand side of the double inequality (or the upper bound on $I^w_{u,v}(t)$) represents the supremum of all possible mutual WiFi interference values. Note that when $x^t_{uk} = x^t_{vh} = 1$, with $c_{kh} = 0$ (u and v are assigned 2 orthogonal channels), the interference is null, $I^w_{u,v}(t) = 0$. In contrast, when $x^t_{uk} = x^t_{vh} = 1$, and $c_{kh} > 0$ (u and v are assigned the same channel or two overlapping channels), $I^w_{u,v}(t)$ accounts for the amount of wasted spectrum of two overlapping channels.

Similarly, let $I^z_{u,v}(t)$ represent the *worst* mutual interference in epoch t between conflicting links (u and v) that use ZigBee protocol. Such interference, $\forall t \in \mathcal{T}, \forall (u,v) \in \mathcal{E}^z_c(t)$, varies as follows:

$$0 \leq I^z_{u,v}(t) \leq \sup_{k \in \mathcal{K}_z} \{y^t_{uk} + y^t_{vk} - 1\} \tag{2}$$

Conversely, $I^{wz}_{u,v}(t)$ represents the *worst* amount of cross technology interference in epoch t due to simultaneous transmissions on interfering links (u and v) established using different protocols. $I^{wz}_{u,v}(t)$, $\forall t \in \mathcal{T}, \forall (u,v) \in \mathcal{E}^{wz}_c(t)$, depends on the binary decision variables x^t_{uk} and y^t_{vh}, and is given by:

$$0 \leq I^{wz}_{u,v}(t) \leq \sup_{k \in \mathcal{K}_w, h \in \mathcal{K}_z} \{a_{kh} \cdot (x^t_{uk} + y^t_{vh} - 1)\} \tag{3}$$

Hence, the total temporal cross-technology interference (CTI) is defined as follows:

$$I(t) = \alpha \cdot \sum_{(u,v) \in \mathcal{E}^w_c(t)} I^w_{(u,v)}(t) + \beta \cdot \sum_{(u,v) \in \mathcal{E}^z_c(t)} I^z_{(u,v)}(t) + \\ + \gamma \cdot \sum_{(u,v) \in \mathcal{E}^{wz}_c(t)} I^{wz}_{(u,v)}(t) \tag{4}$$

and it represents the weighted sum of the three contributions to CTI. The parameters α, β and γ permit to weight differently the three types of interference. Our objective is to minimize the maximum cross-technology interference generated by data transmissions using different technologies on the same available spectrum throughout all epochs. Therefore we define a new variable u that represents the bound on the interference minimized in our model:

$$u \geq I(t), \forall t \in \mathcal{T}. \tag{5}$$

To force the assignment of a single WiFi channel to any wireless link established between two mobile terminals, and the utilization of a single ZigBee channel within a WBAN, we introduce the following constraints:

$$\sum_{k \in \mathcal{K}_w} x^t_{uk} = 1, \forall t \in \mathcal{T}, \forall u \in \mathcal{L}_w(t) \tag{6}$$

$$\sum_{h \in \mathcal{K}_z} y^t_{uh} = 1, \forall t \in \mathcal{T}, \forall u \in \mathcal{L}_z. \tag{7}$$

Indeed, this set of constraints prevents the assignment of multiple channels to a single WiFi or ZigBee interface.

Furthermore, to obtain channel assignments x^t_{uk} and y^t_{uk} that minimize the worst interference generated by simultaneous transmissions throughout all epochs, we define the two following sets of constraints that force the utilization of only one channel for WiFi and ZigBee links in all time epochs:

$$x^t_{uk} = x^{t+1}_{uk}, \forall t \in \mathcal{T}', \forall u \in \mathcal{L}_w(t), \forall k \in \mathcal{K}_w \tag{8}$$

$$y^t_{uh} = y^{t+1}_{uh}, \forall t \in \mathcal{T}', \forall u \in \mathcal{L}_z, \forall h \in \mathcal{K}_z. \tag{9}$$

For the sake of constraints' consistency, in the set $\mathcal{T}'$ we omit the last epoch of $\mathcal{T}$. We observe that by neglecting these two sets of constraints, we can easily model the Channel Switching (CS) to account for devices that can select different frequencies between consecutive time epochs. Indeed, constraints (8) and (9) allow us to significantly reduce the signaling overhead caused by switching channels from one time epoch to another and coordinating mobile devices. Such overhead can become critical and substantial in a dynamic environment, like BBNs.

In this work, since we are assuming that mobile terminals are equipped with only one WiFi interface, we must assign the same wireless channel to all WiFi links established within the same BBN in order to create a multi-hop topology that guarantees the connectivity between any pair of devices. Therefore, we explicitly model connectivity among devices that belong to the same BBN using a set of constraints that forces the utilization of the same channel for any pair of WiFi links that belong to the same BBN:

$$b_{uv}(x^t_{uk} - x^t_{vk}) = 0, \forall t \in \mathcal{T}, \forall u, v \in \mathcal{L}_w(t), \forall k \in \mathcal{K}_w. \tag{10}$$

It is easy to verify that $b_{uv} = 1 \Rightarrow \exists k \in \mathcal{K}_w : x^t_{vk} = x^t_{uk} = 1$.

Given the above definitions and notations, the optimal Cross Technology Interference Mitigation (CTIM) problem can be stated as follows:

$$\begin{aligned}
&\min\ u \\
&\text{s.t.} \\
&\quad u \geq I(t) && \forall t \in \mathcal{T} \\
&\quad \sum_{k \in \mathcal{K}_w} x^t_{uk} = 1 && \forall t \in \mathcal{T}, \forall u \in \mathcal{L}_w(t) \\
&\quad b_{uv}(x^t_{uk} - x^t_{vk}) = 0 && \forall t \in \mathcal{T}, \\
&&& \forall u, v \in \mathcal{L}_w(t), \forall k \in \mathcal{K}_w \\
&\quad \sum_{h \in \mathcal{K}_z} y^t_{uh} = 1 && \forall t \in \mathcal{T}, \forall u \in \mathcal{L}_z \\
&\quad x^t_{uk} = x^{t+1}_{uk} && \forall t \in \mathcal{T}', \\
&&& \forall u \in \mathcal{L}_w(t), \forall k \in \mathcal{K}_w \\
&\quad y^t_{uh} = y^{t+1}_{uh} && \forall t \in \mathcal{T}', \\
&&& \forall u \in \mathcal{L}_z, \forall h \in \mathcal{K}_z \\
&\quad I^w_{u,v}(t) \geq c_{kh} \cdot (x^t_{uk} + x^t_{vh} - 1) && \forall t \in \mathcal{T}, \forall (u,v) \in \mathcal{E}^w_c(t), \\
&&& \forall k, h \in \mathcal{K}_w
\end{aligned}$$

$$I^z_{u,v}(t) \geq y^t_{uk} + y^t_{vk} - 1 \qquad \forall t \in \mathcal{T}, \forall k \in \mathcal{K}_z, \forall (u,v) \in \mathcal{E}^z_c(t)$$

$$I^{wz}_{u,v}(t) \geq a_{kh} \cdot (x^t_{uk} + y^t_{vh} - 1) \qquad \forall t \in \mathcal{T}, \forall (u,v) \in \mathcal{E}^{wz}_c(t), \forall k \in \mathcal{K}_w, \forall h \in \mathcal{K}_z$$

$$x^t_{uk} \in \{0,1\} \qquad \forall t \in \mathcal{T}, \forall u \in \mathcal{L}_w(t), \forall k \in \mathcal{K}_w$$

$$y^t_{vh} \in \{0,1\} \qquad \forall t \in \mathcal{T}, \forall v \in \mathcal{L}_z, \forall h \in \mathcal{K}_z. \quad (11)$$

V. Heuristic Solutions for the CTIM Problem

The CTIM problem is NP-hard. Indeed, it can be demonstrated that the *Maximum K-Cut* problem can be reduced in polynomial-time to the CTIM problem [18]. Finding the optimal solution is thus extremely time consuming, especially in large-scale, real network scenarios composed of several BBNs, as those analyzed in our numerical evaluation. Motivated by this observation, we now present three heuristic approaches to efficiently solve (i.e., in polynomial time) the CTIM problem.

We set out by presenting the first algorithm based on a modified version of the Randomized Rounding (RR) technique. Then, we illustrate the Tabu-Search (TS) solution, and finally we describe the Sequential Fixing (SF) algorithm.

A. RR-CTIM: Randomized Rounding Algorithm

Algorithm 1 illustrates the main steps of the first heuristic solution, which is based on a modified version of the randomized rounding approach. The algorithm receives as input the parameters that describe the network topology, the conflict graph, and the available wireless channels. It produces as output the channel assignment for all BBNs' communication links, which are based either on WiFi or ZigBee technologies.

The algorithm proceeds in three steps. Step 1 solves a continuous relaxation of the CTIM problem, where the integrality constraints of (11) are replaced with their corresponding continuous relaxations. Let $\hat{\boldsymbol{x}}$ and $\hat{\boldsymbol{y}}$ be the optimal relaxed solutions. Steps 2 and 3 perform the randomized rounding on assignment variables $\hat{\boldsymbol{x}}$ and $\hat{\boldsymbol{y}}$, respectively.

Specifically, for WiFi links (step 2), we consider the set that contains all variables $\hat{x}^t_{vk}$ corresponding to possible channels assigned to all links of the same BBN (i.e., the set B_u). From this set, we select the variable with the highest value $x^{t_m}_{i_m k_m}$. We then compare such variable with a random value p that is uniformly distributed in $[0,1]$: if $x^{t_m}_{i_m k_m} \leq p$, all links using the WiFi technology within the same BBN are tuned to the same channel k_m throughout all time epochs, by forcing all variables $x^t_{vk_m} = 1, \forall v \in B_u, \forall t \in \mathcal{T}$ (the remaining variables are set to zero, i.e., $x^t_{vk} = 0, \forall v \in B_u, \forall t \in \mathcal{T}, k \in \mathcal{K}_w, k \neq k_m$).

Regarding the ZigBee channel assigned to the representative link of a WBAN in step 3, we adopt a similar approach, considering the most likely assignment of a ZigBee channel to a WBAN obtained from the relaxed CTIM problem. However, in this latter case, we can perform the randomized rounding of each variable $\hat{y}^t_{uk}$ by forcing only the utilization of the same channel within a WBAN throughout all epochs, since each element $u \in \mathcal{L}_z$ corresponds to an independent WBAN.

Finally, in steps 4 and 5, we verify the feasibility of the solution $(\boldsymbol{x}, \boldsymbol{y})$ provided by the previous operations, ensuring that only one channel is assigned to any wireless link (i.e., constraints (6) and (7)) and that all WiFi links of the same BBN use the same channel (i.e., constraints (10)).

Algorithm 1: RR-CTIM

Input : $\mathcal{N}, G_c(\mathcal{V}_c(t), \mathcal{E}_c(t)), \mathcal{K}_w, \mathcal{K}_z, \boldsymbol{B}, \boldsymbol{C}$
Output: $\boldsymbol{x}, \boldsymbol{y}$

1 $(\hat{\boldsymbol{x}}, \hat{\boldsymbol{y}}) \Leftarrow$ Solve the LP relaxation of the model (11);
$p \Leftarrow rand(0,1)$;
2 **foreach** $u \in \mathcal{L}_w(t)$ **do**
  $B_u \Leftarrow \{v \in \mathcal{L}_w(t) : b_{uv} = 1\}$;
  $x^{t_m}_{i_m k_m} \Leftarrow \max\{\hat{x}^t_{vk} : v \in B_u, k \in \mathcal{K}_w, t \in \mathcal{T}\}$;
  if $x^{t_m}_{i_m k_m} \leq p$ **then**
    foreach $v \in B_u, t \in \mathcal{T}$ **do**
      $x^t_{vk_m} \Leftarrow 1$;
    end
  end
end
$p \Leftarrow rand(0,1)$;
3 **foreach** $u \in \mathcal{L}_z$ **do**
  $y^{t_m}_{uk_m} \Leftarrow \max\{\hat{y}^t_{uk} : k \in \mathcal{K}_z, t \in \mathcal{T}\}$;
  if $y^{t_m}_{uk_m} \leq p$ **then**
    foreach $t \in \mathcal{T}$ **do**
      $y^t_{uk_m} \Leftarrow 1$;
    end
  end
end
4 $\boldsymbol{x} \Leftarrow FeasWiFiSol(\hat{\boldsymbol{x}}, \boldsymbol{x}, G_c(\mathcal{V}_c(t), \mathcal{E}_c(t)), \mathcal{K}_w, \boldsymbol{B}, \boldsymbol{C})$;
5 $\boldsymbol{y} \Leftarrow FeasZigBeeSol(\hat{\boldsymbol{y}}, \boldsymbol{y}, G_c(\mathcal{V}_c(t), \mathcal{E}_c(t)), \mathcal{K}_z)$;

B. TS-CTIM: Tabu-Search Algorithm

To solve the CTIM problem, we develop an efficient heuristic (named TS-CTIM) that uses the tabu-search approach [19] along with polynomial size neighborhoods.

Given a feasible solution f to (11) (i.e., a solution that satisfies all its constraints), the neighborhood is generated by applying the procedure $move$ that proceeds as follows: let h denote the (WiFi or ZigBee) channel assigned to a wireless link u in the current solution f (i.e., $x^t_{uh} = 1$), $move$ will assign a new channel k to u such that k is different from h (i.e., $x^t_{uk} = 1$). More specifically, we develop two different versions of TS-CTIM (TS-CTIM-1 and TS-CTIM-2), which correspond to two different ways of generating and searching the neighborhood of an intermediate solution. Their corresponding neighborhoods are denoted by Neighborhood-1 and Neighborhood-2.

TS-CTIM takes as input parameters the set of mobile terminals $\mathcal{N}$, the conflict graph $G_c(\mathcal{V}_c(t), \mathcal{E}_c(t))$, an initial solution $f_0 = (x_0, y_0)$, the maximum number of iterations nb_iter_max, the size of the tabu list L, the number r of neighboring solutions, and the version (v) of the algorithm used to generate the neighborhood. Based on our tests, we fix the $L = 100$ and $nb\_iter\_max = 20$, since they provide the best trade-off in terms of optimality gap and computational time. The TS-CTIM algorithm produces as output the best solution f_{best} that has been found among those analyzed. To this end, the algorithm starts from a random initial solution $f_0 = (x_0, y_0)$, wherein each wireless (WiFi and ZigBee) link is assigned a channel. The two vectors $\boldsymbol{x}_0$ and $\boldsymbol{y}_0$ represent, respectively, the initial WiFi link-channel assignment and ZigBee link-channel assignment variables' values. The current solution f_i is set to f_0.

The first version of the tabu-search algorithm, TS-CTIM-1, generates at each iteration a sequence of $r^2 + r$ solutions according to the following procedure. Given the current solution $f_i = (x_i, y_i)$, the function *Neighborhood-1*(f_i) first executes one time the $move$ operation on x_i to obtain a neighboring solution (x'_i, y_i). Then, it performs $move$ on y_i, generating r neighboring solutions (x_i, y'_i). Among all these $r + 1$ solutions, the algorithm selects the one with the lowest interference as the new solution (x'_i, y'_i). This is repeated r times (step 3). Among all $r^2 + r$ solutions (x'_i, y'_i), we use the one with the minimum interference as a starting solution for the successive iteration of the TS-CTIM algorithm, $f_i = (x'_i, y'_i)$, with i updated to $i+1$. The algorithm stops after nb_iter_max consecutive iterations without improvement on CTI.

Conversely, the second version of the tabu-search (i.e., TS-CTIM-2), executes the following procedure. First, it applies the $move$ operation on the set of variables representing ZigBee links, y_i, producing a new solution (x_i, y'_i) in which only one channel of a randomly selected ZigBee link is modified. Then, the $move$ operation is applied r times on the set of WiFi links, x_i, to generate r nearby solutions (x'_i, y'_i). In order to modify the assigned channel of r ZigBee links, the previous procedure is executed r times, resulting in a set of $r^2 + r$ solutions explored at each iteration.

Both alternative versions of the TS-CTIM algorithm terminate after nb_iter_max consecutive iterations that result in no improvement in the CTI. Indeed, every time a solution f_i produces a lower cross-technology interference $CTI(f_i)$, the iterations counter i is reset to avoid local minima (step 4). A formal description of the TS-CTIM algorithm (i.e., TS-CTIM-1 and TS-CTIM-2) is provided in Algorithm 2.

Algorithm 2: TS-CTIM

Input : $\mathcal{N}, G_c(\mathcal{V}_c(t), \mathcal{E}_c(t)), f_0 = (\boldsymbol{x}_0, \boldsymbol{y}_0), nb\_iter\_max, L, r, v$
Output: $\boldsymbol{x_{best}}, \boldsymbol{y_{best}}$

1 Start with an initial solution $f_0 = (x_0, y_0)$;
$i = 0$, $k = 0$, $f_{best} = f_0$, $I_{best} = CTI(f_0)$;
2 **while** $i < nb\_iter\_max$ **do**
3 **while** $k < r$ **do**
$F_i \Leftarrow$Neighborhood-v(f_i);
$f_i \Leftarrow argmin_{\boldsymbol{F_i}} I(t)$;
Add $move(f_i)$ to the tabu list;
$k \Leftarrow k + 1$;
end
4 **if** $(CTI(f_i) \leq I_{best})$ **then**
$f_{best} \Leftarrow f_i$;
$I_{best} \Leftarrow CTI(f_i)$;
$i \Leftarrow 0$;
else
$i \Leftarrow i + 1$;
end
end
5 Return $f_{best} = (\boldsymbol{x_{best}}, \boldsymbol{y_{best}})$;

C. LPSF-CTIM: Linear Programming with Sequential Fixing Algorithm

We exploit the structure of our problem to develop a polynomial-time approximate algorithm, called Linear Programming with Sequential Fixing Cross-Technology Interference Mitigation (LPSF-CTIM) algorithm. In Theorem V.1, we show that LPSF-CTIM always converges to an integer solution. The technique of Sequential Fixing (SF) has been proven to be very efficient in solving classical channel assignment problems [20], [21], and hence this technique is extended to our CTIM problem, and applied to WiFi channel assignment variables, and then to ZigBee variables.

The LPSF-CTIM algorithm, listed as Algorithm 3, proceeds as follows. In step 1, we relax the binary variables x^t_{uk} and y^t_{vh} of the Integer Programming CTIM problem to obtain the LP relaxed version (denoted as LP-CTIM), whose optimal solution can be computed in polynomial-time. Then, in step 2, we solve LP-CTIM to obtain such an optimal real-valued solution $\hat{x}^t_{uk}$ and $\hat{y}^t_{vh}$. The third step of LPSF-CTIM aims at choosing among all $\hat{x}^t_{uk}$ the one with the largest real value, denoted hereafter by $x^{t_m}_{u_m k_m}$, and setting its value to 1. Once $x^{t_m}_{u_m k_m}$ is determined, step 3 performs the following operations:

- Set all variables $x^{t_m}_{u_m k}$ to zero, where $k \neq k_m$ (since wireless link u_m must be assigned a single WiFi channel according to constraints (6)).
- Set all $x^t_{uk_m}$ to 1 if link u belongs to the same BBN of u_m. As a consequence, u and u_m must be assigned the same channel to ensure WiFi connectivity between WBANs of the same BBN (constraints (10)).

After identifying the WiFi variable $x^{t_m}_{u_m k_m}$, we reformulate the problem LP-CTIM^{x,1} forcing $x^{t_m}_{u_m k_m}$ equal to 1 and all other variables modified as described in previous steps (step 4). If the LP-CTIM^{x,1} problem is feasible, we redefine LP-CTIM equal to LP-CTIM^{x,1}. Otherwise, we reformulate another LP problem, LP-CTIM^{x,0}, by fixing $x^{t_m}_{u_m k_m}$ and all the variables $x^{t_m}_{uk_m}$ (where u belongs to the same BBN of u_m) to zero. Then, we redefine LP-CTIM equal to LP-CTIM^{x,0}. The algorithm iterates through steps 2 to 5 until all WiFi channel assignment variables, $\boldsymbol{x}$, are fixed.

In a similar way, we apply the above procedure to the variables representing the ZigBee channel assignment, y^t_{vh}. Specifically, we formulate the problem LP-CTIM^{y,1} by fixing $y^{t_m}_{v_m h_m} = 1$ in LP-CTIM (step 8), and we set all variables $y^{t_m}_{v_m h}$, $\forall h \neq h_m$ equal to 0, since only one channel must be assigned to any wireless link v_m. If LP-CTIM^{y,1} results in an infeasible solution, we switch the value assigned to the variable $y^{t_m}_{v_m h_m}$, defining the corresponding problem as LP-CTIM^{y,0}. At this point, we either have a feasible LP-CTIM^{y,1} or a feasible LP-CTIM^{y,0}. Hence, the algorithm iterates again through steps 7 and 9 until all ZigBee channel assignment variables, y^t_{vh}, are fixed. Finally, the LPSF-CTIM algorithm terminates and returns the solution of WiFi and ZigBee channel assignments.

In the following, we prove by induction that the LPSF-CTIM algorithm converges in polynomial time to an integer solution.

Theorem V.1. *For each time epoch $t \in \mathcal{T}$, the LPSF-CTIM algorithm can determine the values of all binary variables $\boldsymbol{x}$ and $\boldsymbol{y}$ in no more than $|\mathcal{L}_w||\mathcal{K}_w| + |\mathcal{L}_z||\mathcal{K}_z|$ iterations.*

Proof: The proof of Theorem V.1 is based on the following

Algorithm 3: LPSF-CTIM

Input : $\mathcal{N}, G_c(\mathcal{V}_c(t), \mathcal{E}_c(t)), \mathcal{K}_w, \mathcal{K}_z, \boldsymbol{B}, \boldsymbol{C}$
Output: $\boldsymbol{x}, \boldsymbol{y}$

LP-CTIM $\Leftarrow$ LP version of (11), $x_{uk}^t \in [0,1]$ and $y_{vh}^t \in [0,1], \forall t \in \mathcal{T}, u \in \mathcal{L}_w(t), v \in \mathcal{L}_z, k \in \mathcal{K}_w, h \in \mathcal{K}_z$.
while *not all* $\boldsymbol{x}$ *are fixed* **do**
  $(\hat{\boldsymbol{x}}, \hat{\boldsymbol{y}}) \Leftarrow$ Solve LP-CTIM;
  $x_{u_m k_m}^{t_m} \Leftarrow \max\{\hat{x}_{uk}^t : u \in \mathcal{L}_w(t), k \in \mathcal{K}_w, t \in \mathcal{T}\}$;
  $x_{u_m k_m}^{t_m} = 1$ and $x_{u_m k}^{t_m} = 0, \forall k \in \mathcal{K}_w, k \neq k_m$;
  $x_{uk_m}^{t} = 1, \forall u \in B_{u_m}$;
  LP-CTIM$^{x,1} \Leftarrow$ LP-CTIM with $x_{u_m k_m}^{t_m} = 1$ and $\forall\ x$ and y already fixed in step 3;
  if *LP-CTIM*^{x,1} *is feasible* **then**
    LP-CTIM $\Leftarrow$ LP-CTIM^{x,1};
  else
    Define LP-CTIM^{x,0} as LP-CTIM with $x_{u_m k_m}^{t_m} = 0$ and $x_{uk_m}^{t_m} = 0, \forall u \in B_{u_m}$;
    LP-CTIM $\Leftarrow$ LP-CTIM^{x,0};
  end
end
while *not all* $\boldsymbol{y}$ *are fixed* **do**
  $(\hat{\boldsymbol{x}}, \hat{\boldsymbol{y}}) \Leftarrow$ Solve LP-CTIM;
  $y_{v_m h_m}^{t_m} \Leftarrow \max\{\hat{y}_{vh}^t : v \in \mathcal{L}_z, h \in \mathcal{K}_z, t \in \mathcal{T}\}$;
  LP-CTIM$^{y,1} \Leftarrow$ LP-CTIM with $y_{v_m h_m}^{t_m} = 1$ and $y_{v_m h}^{t_m} = 0, \forall h \in \mathcal{K}_z, h \neq h_m$;
  if *LP-CTIM*^{y,1} *is feasible* **then**
    LP-CTIM $\Leftarrow$ LP-CTIM^{y,1};
  else
    Define LP-CTIM^{y,0} as LP-CTIM with $y_{v_m h_m}^{t_m} = 0$;
    LP-CTIM $\Leftarrow$ LP-CTIM^{y,0};
  end
end
Return $(\boldsymbol{x}, \boldsymbol{y})$;

lemmas.

Lemma V.2. *In the first iteration, LP-CTIM has a nonempty feasible solution set, and its variables are bounded (*$0 \leq x_{uk}^t, y_{vh}^t \leq 1$*). Hence, it has an optimal solution.*

Proof: It is easy to check that the solution obtained assigning the WiFi channel 1 to all WiFi links and the ZigBee channel 16 to all ZigBee links[2], i.e., $x_{u1}^t = 1, \forall u \in \mathcal{L}_w(t), t \in \mathcal{T}$, $x_{uk}^t = 0, \forall u \in \mathcal{L}_w(t), t \in \mathcal{T}, k \in \mathcal{K}_w$, with $k \neq 1$, and $y_{v16}^t = 1, \forall v \in \mathcal{L}_z, t \in \mathcal{T}$, and $y_{vh}^t = 0, \forall v \in \mathcal{L}_z, t \in \mathcal{T}, h \in \mathcal{K}_z$, with $h \neq 16$, is a feasible solution to the CTIM problem, and as a consequence, to the LP-CTIM problem. Since the feasible solution set of LP-CTIM is nonempty and the variables x_{uk}^t and y_{vh}^t are bounded between 0 and 1, Lemma V.2 holds.

Lemma V.3. *In the first iteration, since LP-CTIM*^{x,0} *has a nonempty feasible solution set and its variables are bounded, it also has an optimal solution.*

Proof: It follows from Lemma V.2 that LP-CTIM in the first iteration must have an optimal solution. Therefore, $x_{u_m k_m}^{t_m}$ is ≥ 0 before performing the fixing. When $x_{u_m k_m}^{t_m}$ and $x_{uk_m}^{t_m}$, $\forall u \in B_{u_m}$ are fixed to 0 while formulating the LP-CTIM^{x,0} problem, none of the constraints of the LP relaxation of (11) could be violated by this decreasing action on the variables' values. In fact, if we substitute $x_{u_m k_m}^{t_m}$ and $x_{uk_m}^{t_m}$, $\forall u \in B_{u_m}$ by 0 in constraints (6), we force all wireless links in BBN B_{u_m} to use a WiFi channel $k \in \mathcal{K}_w$ which is different from k_m; however, LP-CTIM^{x,0} is still feasible, and has at least a feasible solution. Therefore, LP-CTIM^{x,0}, as LP-CTIM, must have at least one feasible solution. Since the feasible solution set of LP-CTIM^{x,0} is nonempty and the variables x_{uk}^t and y_{vh}^t are bounded between 0 and 1, Lemma V.3 holds.

[2]This assignment ensures that there is no overlap between the WiFi and ZigBee channels.

Lemma V.4. *In all iterations, since LP-CTIM and LP-CTIM*^{x,0} *have nonempty feasible solution sets and their variables are bounded, they also have optimal solutions.*

Proof: The existence of an optimal solution for LP-CTIM and LP-CTIM^{x,0} in the first iteration is proved by Lemma V.2 and Lemma V.3, respectively. In the second iteration, LP-CTIM is obtained either from a feasible LP-CTIM^{x,1} or a feasible LP-CTIM^{x,0} of the first iteration. Hence, it must be feasible in the second iteration. Given that LP-CTIM is feasible in the second iteration, the rationale used in proving Lemma V.3 also applies here to prove the feasibility of LP-CTIM^{x,0} in the second iteration. This induction can be repeated in all iterations. Noting that all variables are bounded, Lemma V.4 holds.

Lemma V.5. *In all iterations, since LP-CTIM (step 6 of LPSF-CTIM algorithm) and LP-CTIM*^{y,0} *(step 9) have nonempty feasible solution sets and their variables are bounded, they also have optimal solutions.*

Proof: On one hand, it follows from Lemma V.4 that LP-CTIM (the one defined in step 6), at the first iteration, must be feasible, and according to Lemma V.2 must have one optimal solution since the y_{vh}^t variables are bounded. On the other hand, it follows from Lemma V.3 that at the first iteration LP-CTIM^{y,0} (the problem formulated at step 9) has an optimal solution. Hence, again, according to Lemma V.4 these problems also have optimal solutions in all iterations. Therefore, Lemma V.5 holds.

At this point, the proof of Theorem V.1 is straightforward: By iteratively applying Lemmas V.2 to V.5, it is guaranteed that in each iteration at least one x_{uk}^t, and then one y_{vh}^t, is fixed to either 0 or 1 and a new feasible LP-CTIM problem is generated for the next iteration.

Based on Theorem V.1, it is easy to show that the computational complexity of LPSF-CTIM is bounded by the complexity of the LP solver times $|\mathcal{L}_w(t)||\mathcal{K}_w| + |\mathcal{L}_z||\mathcal{K}_z|$. Since our linear programming problems (LP-CTIM, LP-CTIM^{x,0}, LP-CTIM^{x,1}, LP-CTIM^{y,0}, LP-CTIM^{y,1}) can be solved in polynomial-time, the complexity of the proposed LPSF-CTIM algorithm is polynomial. In addition, as we show in the Numerical Results section, the performance gap between the approximate LPSF and the exact (optimal) solutions can be very small (always below 15%), and in most cases it is null.

VI. Interference Mitigation Protocol

This section presents the design of the signaling protocol necessary to implement our CTI mitigation algorithm in a distributed fashion. We first describe the protocol used by mobile terminals to exchange the proximity information necessary to build the conflict graph. Then, we detail the operations performed by all devices to compute in a completely distributed

fashion the channel assignment that minimizes the maximum CTI, based on local information.

A. Signaling Protocol

In order to update the topology information related to network connectivity, network nodes periodically exchange control messages among each other using a common control channel, similar to *link-state* routing protocols. This information is then used by the interference mitigation algorithm to create the conflict graph and compute the channel assignment that minimizes the cross-technology interference.

In the design of our protocol, we assume that two nodes within their reciprocal interference ranges can communicate with each other. We observe that in scenarios where mobile terminals use a transmission power for intra-WBAN communications that is lower than the power used on the control channel, such an assumption provides a good approximation of the real level of interference. Conversely, to further improve the interference estimation, we can integrate other measures of interference, such as the Link Interference Ratio (LIR) and the Broadcast Interference Ratio (BIR) proposed in [17]. We further note that solutions to the *blind rendezvous problem*, i.e., the problem of establishing communications without a common control channel or a centralized controller (e.g., [22], [23], [24]), can be used to disseminate control messages in our protocol. Moreover, the periodic scanning of the available channels performed by WiFi devices can further simplify the operations necessary to establish communication links among nearby WBANs.

To represent interfering WiFi transmissions with the corresponding conflict edges, each node needs to know the devices within the 1-hop and 2-hop neighbor sets (i.e., nearby nodes whose transmissions can be directly decoded, and nodes that can be reached through direct neighbors). Indeed, assuming the availability of an ARQ (Automatic Repeat reQuest) mechanism to recover from transmission errors caused by noise or collisions, all WiFi transmissions within the 2-hop neighbor set cannot be scheduled simultaneously, since their transmissions are hidden from the transmitter [25]. Conversely, only nodes within the 1-hop neighbor set are considered for the representation of interfering ZigBee links, since transmissions using the ZigBee technology involve only the mobile terminal and sensor nodes within the same WBAN (i.e., two or more different WBANs exchange information among each other through the WiFi technology even if they belong to the same BBN). Therefore, simultaneous transmissions on ZigBee links of two different WBANs whose mobile terminals are more than one hop away do not interfere with each other.

Given the different interference models of the two wireless technologies, we define two different sets of control messages. More specifically, the control traffic related to the WiFi connectivity is exchanged using two different types of messages: *beacon* messages, which permit the discovery of 1-hop and 2-hop neighbors, and *link-state* messages, which are used to disseminate topology information within the network. In contrast, only *beacon* messages are transmitted periodically by ZigBee sensor nodes of a WBAN (either using the mobile terminal interface or directly by any sensor node of the WBAN), since only adjacent WBANs interfere with each other. The content of WiFi beacons differs from that of ZigBee beacons. A WiFi beacon message contains the identifier of the WBAN (concatenation of the addresses of the two radio interfaces of the mobile terminal), and a list of neighbors from which control traffic has been recently received. Each neighbor in the list is represented using its WBAN and the BBN identifiers. This list enables a mobile terminal to detect the nodes that belong to the 2-hop neighbor set. In contrast, the ZigBee beacon message contains only the identifier of the WBAN, since conflicts arise only among adjacent WBANs.

Finally, WiFi *link-state* messages are used to spread topology information to the entire network. A link-state message contains two lists of WiFi and ZigBee neighbors, each identified by its WBAN and BBN identifiers, in addition to the identifier of the underlying WBAN. Such messages are used by devices three or more hops away to build the network topology and the conflict graph.

Figure 3 illustrates a simple network scenario with three BBNs. In this example, the 1-hop neighbor set of mobile terminal 2 is $\mathcal{N}^1(2) = \{1, 3, 7, 8\}$, whereas its 2-hop neighborhood contains only node 4, i.e., $\mathcal{N}^2(2) = \{4\}$.

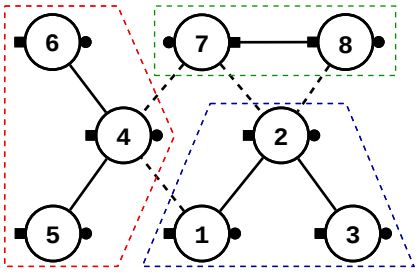

Fig. 3: Neighborhood relationships among BBN nodes.The small squares and circles depict WiFi and ZigBee radio interfaces, respectively. Solid lines represent WiFi links established between 1-hop neighbors of the same BBN, whereas dashed lines show nearby nodes of different BBNs that are detected using WiFi beacon messages.

B. Operational Details

Having described the signaling protocol, we now detail the operations performed by all nodes to build the conflict graph and compute the channel assignment that minimizes the maximum CTI. For simplicity, we omit the index t of the time epoch in the description of the operations.

For the representation of the mutual WiFi interference, each mobile terminal maintains the 1-hop and 2-hop neighbor sets as well as a list containing the links advertised by other nodes in their link-state messages. Upon receiving a *WiFi beacon* or *link-state* message, the interference mitigation algorithm extracts the information necessary to update the network topology and the conflict graph. In particular, for each neighbor $j \in \mathcal{N}^1(i)$, advertised in a *WiFi beacon* by originating node o, that does not belong to the same BBN of the receiving node i, a new vertex (o, j) is added to the conflict graph. Such vertex is connected through a conflict edge to all vertices representing wireless links whose terminating nodes are in the 1-hop neighbor set, i.e., $\forall j, k \in \mathcal{N}^1(i), \exists (e_1, e_2) \in \mathcal{E}_c : e_1 =$

$(i,j), e_2 = (i,k)$, where $\mathcal{N}^1(i)$ is the 1-hop neighbor set of node i. Furthermore, a new conflict edge is established between each link $(i,j) \in \mathcal{L}_w$, which may connect a node $i \in \mathcal{N}$ with one of its neighbors $j \in \mathcal{N}^1(i)$, and any link whose terminating or originating node belongs to the 2-hop neighborhood $k \in \mathcal{N}^2(i)$: $\forall j \in \mathcal{N}^1(i), \forall k \in \mathcal{N}^2(i), \exists (e_1, e_2) \in \mathcal{E}_c : e_1 = (i,j), e_2 = (k,h)$ *or* $e_2 = (h,k)$, where $\mathcal{N}^2(i)$ represents the 2-hop neighbor set. As for links whose end nodes are more than 2 hop away (i.e., $(j,k) \notin \mathcal{N}^1(i) \cup \mathcal{N}^2(i)$), conflict edges are added by controlling/examining the network topology, which is built using the information carried in the link-state messages. We emphasize that the previous rules are applied only to links whose nodes belong to different BBNs, since the unique WiFi radio interface of nodes of the same BBN must be tuned to the same channel.

The modeling of the mutual ZigBee interference requires simpler rules for the generation of the corresponding conflict edges, since only links with one common ZigBee interface interfere with each other. Therefore, for each received *ZigBee beacon* message, the receiving node i extracts the WBAN's identifier j, creates a new ZigBee link $j \in \mathcal{L}_z$ whose corresponding vertex is connected through a conflict edge to all vertices representing incident links, i.e., $\forall j,k \in \mathcal{N}^1(i), \exists (e_1,e_2) \in \mathcal{E}_c : e_1 = j, e_2 = k$. Note that the remaining links and conflict edges can be determined by analyzing link-state messages, which contain the list of adjacent ZigBee WBANs of the message originator.

Finally, for the representation of CTI, each node combines network connectivity information of different technologies, using all received control messages. Specifically, for each WiFi link (i,j), $2+|\mathcal{N}^1(i) \vee \mathcal{N}^1(j)|$ cross-conflict edges are created: the first two edges represent the interference generated across the different radio interfaces of mobile terminals i and j, while the remaining edges model the interference that the WiFi transmitters of i and j cause to the ZigBee receiver of their 1-hop neighbors.

Once a node has collected enough information to build the network topology and the conflict graph, it executes the sequential fixing algorithm presented in Section V-C. Indeed, the distributed execution of LPSF-CTIM using the same information leads all nodes to the same solution, since the algorithm consists of only deterministic operations. Nonetheless, our distributed algorithm always computes a feasible yet sub-optimal channel allocation even if mobile terminals use different information due to fast topology changes [26]. Furthermore, we observe that the iterative version of the sequential fixing approach, which optimizes sequentially over each time epoch, converges to the solution obtained using knowledge of future conflicts, when such information is transmitted faster than network changes. On the contrary, the tabu-search and randomized rounding approaches cannot be executed independently by all nodes, since they contain probabilistic steps.

In order to limit channel updates whenever a new control message is received, nodes switch channels only if the new solution provides a large improvement with respect to the previous channel assignment. To this end, we can integrate a hysteresis mechanism that keeps using the latest channel assignment as long as the variation in the CTI metric $I(t)$ computed by each node is lower than a threshold. Note that such a threshold must be set to select the best trade-off between system performance and overhead. To further reduce the signaling overhead and prevent stale information from reaching distant nodes, we can employ the Fisheye technique [27], defining different transmission periods for WiFi beacon and link-state messages. Using this technique, each node maintains accurate information about the immediate neighborhoods, namely the 1-hop and 2-hop neighbor sets, with progressively less detail as the distance increases.

VII. Numerical Results

This section presents numerical results that illustrate the validity of the proposed algorithms to solve the CTI mitigation problem. More specifically, we evaluate the impact of BBN density (i.e., the total number of WBANs in a BBN) on the performance of the overall system using the algorithms developed in previous sections.

We first describe the experimental methodology of our simulations. We then analyze and discuss the performance achieved by the proposed algorithms.

A. Experimental Methodology

In our simulations, we consider both *static* and *dynamic* BBN topologies whose nodes (the WBANs) are randomly scattered over an area of $500 \times 500 m^2$. Note that we increase the size of the simulation area with respect to our previous paper [28], in order to analyze the performance of our solution in highly dense networks. To evaluate the effect of node density on the level of interference, we vary the total number of mobile terminals in the range $[20, 50]$, similarly to [29]. To do so, we fix the number of mobile terminals within each BBN to 5 and vary the number of BBNs from 4 to 10. Specifically, BBN centers are scattered according to a uniform distribution inside the simulation area, whereas the mobile terminals are deployed around each BBN center according to a bi-dimensional Gaussian distribution with a standard deviation of 100 meters.

In the *dynamic* network scenario, we simulate BBNs' mobility using the random way-point model [30], which is a commonly used mobility model. In particular, for each time epoch we compute the random displacements of all BBNs' centers, and we move all mobile terminals within the same BBN towards the same direction according to the displacement vector.

In our simulations, we consider only the three orthogonal channels defined by the WiFi alliance ($\mathcal{K}_w = \{1,6,11\}$), whereas for the WBAN links we use all the 16 available ZigBee channels ($\mathcal{K}_z \in [11,26]$). The transmission powers of WiFi and ZigBee radio interfaces are fixed to 100 mW and 10 mW, respectively. In order to offset the higher transmission power used by the WiFi technology, which is 10 times greater than the ZigBee transmission power, we set $\gamma = 10$ in Equation (4). Furthermore, we set the coefficients related to the mutual interferences $\alpha = 5$ and $\beta = 1$ so as to penalize more the number of potential WiFi conflicts than those generated by the ZigBee technology.

The conflict graph is computed assuming an ARQ mechanism is in place (i.e., we assume DATA-ACK message exchange between network nodes involved in data communications). The reception and carrier sense thresholds used to decide whether nodes can establish communication links or interfere with each others are defined according to the sensitivity of Atheros (WiFi)[3] and CC2420 (ZigBee)[4] radio chipsets. The path loss, which is necessary to evaluate the sensitivity of the receiving node, is computed according to the Friis propagation model. We emphasize that all above assumptions do not affect the proposed algorithms, which are general and can be used to solve any network scenario.

In order to gauge the performance of the proposed heuristic algorithms (Section V) with respect to the optimal solution (Section IV), we consider the CTI as defined in (4) and the normalized throughput. Furthermore, in the *dynamic* scenario, we measure the number of times different channels are assigned to ZigBee links across two consecutive epochs, since this number provides an indication of the signaling overhead needed to coordinate channel switching.

Note that due to the high computational and storage complexities of the ILP model, we could not scale beyond the network sizes and time epochs discussed above (i.e., 50 nodes and 10 time epochs).

B. Performance Evaluation

1) Static Scenario: We first evaluate the effect of node density and the number of available channels on the performance of our interference mitigation techniques. Specifically, we vary the number of mobile terminals in the range $[20, 50]$ and we progressively increase the number of orthogonal WiFi channels from 1 to 3. Figure 4 shows the CTI obtained using our proposed algorithms. TS-CTIM-1 and 2 take as an initial solution the one given by the RR algorithm to further improve this solution and obtain a final good solution. For the sake of clarity, the CTI has been normalized with respect to the maximum value measured by the RR-CTIM algorithm.

The curves identified by labels "Opt.", "RR", "TS-v" ($v \in \{1, 2\}$), and "SF" illustrate, respectively, the performance metrics computed using the optimal, the randomized rounding, the two tabu-search, and the sequential fixing algorithms.

As illustrated in the figures, the two versions of the tabu-search algorithm and the sequential fixing scheme approach the optimal solution, whereas the randomized rounding technique always provides solutions with higher interference. We observe that in almost all network instances, the decision variables of the LP relaxation have almost the same values, which are interpreted by the RR-CTIM algorithm as an even channel assignment, thus failing to drive effectively the remaining operations of the algorithm. Indeed, when the optimal solution of the LP relaxation provides the same values to all decision variables, the $FeasWiFiSol()$ and $FeasZigBeeSol()$ functions in Algorithm 1 generate random channel assignment to WiFi and ZigBee links.

[3]Available online at http://www.diswire.com/SpecsCM9.pdf

[4]Available online at http://www.ti.com/lit/ds/symlink/cc2420.pdf

As expected, increasing node density within the simulation area leads to higher CTI, since the mobile terminals and the sensor devices of the WBANs get closer, thus increasing the number of edges in the conflict graph. It can be further observed from Figures 4(a), 4(b) and 4(c) that the number of available WiFi channels affects the performance of all approaches. Specifically, the higher the number of orthogonal channels, the lower is the overall interference of the solution computed by the optimal, tabu-search, and sequential fixing algorithms. Furthermore, as illustrated in Figures 4(b) and 4(c), LPSF provides better performance than TS-CTIM-1 and TS-CTIM-2, since the subset of the solution space explored by the SF procedure is better than the solutions analyzed by the tabu-search approaches. Indeed, TS-CTIM-1 and TS-CTIM-2 start from the solution provided by the RR algorithm, which causes the worst level of interference.

In order to gauge the improvement offered by the SF approach over the other heuristics and demonstrate how the CTI metric enables objective assessment of the performance enhancements relative to the standard AFH scheme, we measure the average normalized throughput of WiFi ($\overline{\rho^w}$) and ZigBee ($\overline{\rho^z}$) links as follows:

$$\overline{\rho^w} = \frac{1}{|\mathcal{T}|} \sum_{t \in \mathcal{T}} \frac{1}{|\mathcal{L}_w(t)|} \sum_{u \in \mathcal{L}_w(t)} \rho_u^w(t) \tag{12}$$

$$\overline{\rho^z} = \frac{1}{|\mathcal{T}| \cdot |\mathcal{L}_z|} \sum_{t \in \mathcal{T}} \sum_{u \in \mathcal{L}_z} \rho_u^z(t). \tag{13}$$

Assuming backlogged traffic and a slotted TDMA coordination mechanism, the normalized throughput $\rho_u^w(t)$ that can be achieved by a WiFi link $u \in \mathcal{L}_w$ at time epoch $t \in \mathcal{T}$ is:

$$\rho_u^w(t) = \frac{1}{1 + w_u^m(t) + w_u^c(t)} \tag{14}$$

where $w_u^m(t) = \sum_{\substack{v \in \mathcal{L}_w(t): \\ (u,v,t) \in \mathcal{E}_c^w(t)}} I_{u,v}^w(t)$ and $w_u^c(t) = \sum_{\substack{v \in \mathcal{L}_z: \\ (u,v,t) \in \mathcal{E}_c^{wz}(t)}} I_{u,v}^{wz}(t)$ represent the number of links that interfere with link u using non-orthogonal WiFi and ZigBee channels, respectively. Note that the normalized throughput calculated using a slotted TDMA system provides an upper bound on the real throughput that can be achieved in realistic BBN scenarios. Nonetheless, the performance gap measured in our numerical analysis among our different approaches remains likely similar to that we can obtain in more realistic settings.

Similarly, the normalized throughput $\rho_u^z(t)$ that can be achieved by ZigBee link $u \in \mathcal{L}_z$ at time $t \in \mathcal{T}$ is given by:

$$\rho_u^z(t) = \frac{1}{1 + z_u^m(t) + z_u^c(t)} \tag{15}$$

where $z_u^m(t)$ and $z_u^c(t)$ represent the number of ZigBee links and the number of WiFi links that interfere with ZigBee link u, respectively.

Figures 6(a) - 6(b) show the normalized throughput for WiFi and ZigBee links as a function of the number of mobile terminals in the static network scenario with three orthogonal WiFi channels. It can be observed that the minimization of the CTI results in the improvement of the WiFi and ZigBee throughput, and both the optimal and sequential fixing solutions favor ZigBee over WiFi transmissions. Indeed, they select WiFi channel assignments that achieve slightly worse performance

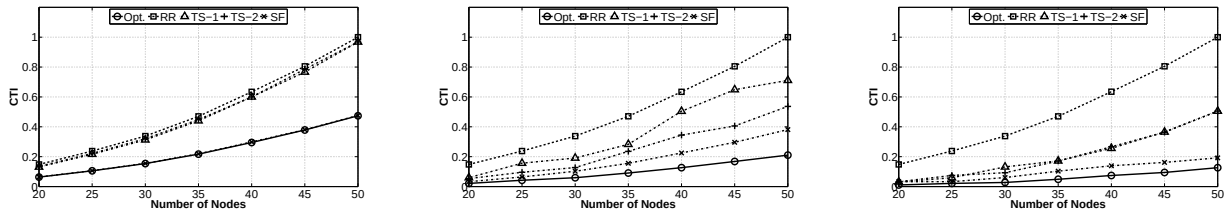

(a) 1 WiFi Channel (b) 2 WiFi Channels (c) 3 WiFi Channels

Fig. 4: Cross-technology interference as a function of node density and number of orthogonal WiFi channels (i.e., $\{1, 6, 11\}$) in the *static* network scenario. All results are normalized to the maximum CTI computed using the RR-CTIM algorithm ($I(t) \simeq 46000$).

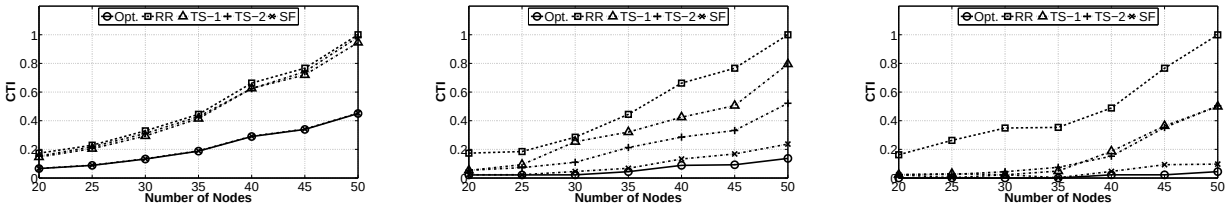

(a) 1 WiFi Channel (b) 2 WiFi Channels (c) 3 WiFi Channels

Fig. 5: Cross-technology interference as a function of node density and number of orthogonal WiFi channels (i.e., $\{1, 6, 11\}$) in the *dynamic* network scenario. All results are normalized to the maximum CTI computed using the RR-CTIM algorithm ($I(t) \simeq 16000$).

(a) WiFi Throughput (b) ZigBee Throughout

Fig. 6: Average normalized throughput of WiFi and ZigBee links as a function of the number of mobile terminals (static network scenario with three WiFi channels).

than tabu-search heuristics in order to reserve more spectrum for ZigBee communications. We underline that WiFi technology achieves higher transmission rates than ZigBee (up to more than 3 orders of magnitude). Therefore, any algorithm for mitigating cross-technology interference should allocate the available spectrum in a way to privilege ZigBee transmissions, whenever such transmissions are deemed essential for the correct operation of the BBN system.

2) Dynamic Scenario with Fixed Channels: The second set of simulated scenarios, whose results are depicted in Figure 5, aims at evaluating the effect of the mobility on the performance of our proposed schemes. To this end, within the $500 \times 500m^2$ simulation area, we randomly move all nodes throughout 10 time epochs according to the mobility model described before. The mobile terminal speed is set to 1 meter/sec, while the duration of one time epoch is fixed to 10 seconds. This time is long enough to capture significant changes in both network topology and the conflict graph. As in the *static* scenario, the CTI has been normalized with respect to the maximum value measured by the RR-CTIM algorithm.

The results obtained in the dynamic scenario confirm the trends observed in the static scenario. Specifically, the CTI improves by increasing the number of orthogonal WiFi channels and decreasing node density (or equivalently by increasing the spatial reuse). Since the number of orthogonal WiFi channels in the ISM band is limited, BBNs' users should improve the spatial reuse, reducing the transmission power to the minimum level necessary to maintain network connectivity. Finally, we can observe that node density affects the network performance more than mobility, since all algorithms minimize the worst CTI throughout all time epochs.

We further evaluate the computational time required to solve the CTIM problem optimally and also using our heuristic approaches. The results are illustrated in Table I. As expected, the execution time for the optimal algorithm increases exponentially with the number of nodes. On the contrary, the execution time of the RR-CTIM and LPSF-CTIM heuristics increases linearly with the network size. LPSF-CTIM takes a longer time than RR-CTIM to find a solution, since it solves an instance of the relaxed problem for each decision variable. Note, however, that the iterative version of the LPSF-CTIM algorithm, which solves the problem considering sequentially each time epoch, takes always less than 6 seconds. Furthermore, we can speed up the computation of LPSF-CTIM by fixing the channel assigned to all WiFi links of a BBN whenever any variable x_{uk}^t is fixed to one, according to constraint (10). Numerical results also confirm that the computational time of TS-CTIM-1 and TS-CTIM-2 slightly varies with the number of nodes. Indeed, the computational complexity of tabu-search approaches is mainly affected by the tabu-list, the neighborhood size, and the maximum number of iterations rather than the network size.

3) Dynamic Scenario with Channel Switching: To provide further insight into the gain achievable by enabling the channel switching, we evaluate the performance in terms of the signaling overhead incurred by various algorithms, neglecting constraints (8) and (9) for the optimization based approaches and optimizing the topologies of all time epochs as

TABLE I: Computational Time for solving the CTIM problem (s)

2 WiFi Channels							
Nodes	20	25	30	35	40	45	50
Opt.	2.5	4	7.5	13	32	83	237
RR	1.61	2.76	3.72	5.17	7.05	8.80	11.1
TS-1	1.15	1.20	1.24	1.27	1.32	1.36	1.42
TS-2	1.16	1.20	1.24	1.28	1.33	1.36	1.42
SF	4	9	15	24	33	47	56
3 WiFi Channels							
Nodes	20	25	30	35	40	45	50
Opt.	4.7	12	37	98	278	1704	51338
RR	2.26	3.61	5.13	7	9.25	11.8	14.76
TS-1	1.16	1.20	1.24	1.28	1.33	1.36	1.42
TS-2	1.17	1.20	1.24	1.28	1.34	1.37	1.42
SF	5	10	18	27	38	55	64

consecutive instances of the static scenario for the tabu-search and sequential fixing approaches. Recall that by ignoring constraints (8) and (9), the model enables wireless links to change channel at different time epochs. In particular, we illustrate the distribution of ZigBee links that switch channels during the simulation time and the overall number of channels used by various algorithms. Note that the modified algorithms to consider the channel switching functionality achieve the same maximum CTI shown in Figure 5.

Figure 7 shows the distribution of ZigBee links that switch channels, obtained under the optimal and heuristic algorithms. The network scenario consists of 40 mobile terminals and 3 WiFi channels. For the sake of brevity, we do not illustrate the results obtained with fewer mobile terminals (the distributions depict similar trends, but with a smaller average number of channel changes). Even though the optimal algorithm achieves the lowest CTI, all ZigBee links change their channels at least four times, as illustrated in Figure 7. The percentage of links that switch channels at least four times decreases by 95% for the tabu-search approaches ($\mathcal{F}(x \geq 4) = 0.05$), 85% for the sequential fixing algorithm, and 10% using the randomized rounding scheme. This is mainly due to the smaller solution space analyzed by the heuristic and sequential fixing approaches, which indirectly requires lower channel changes than the optimal algorithm. Indeed, we noticed that the randomized rounding approach selects almost uniformly the channels assigned to each epoch, while the generation of the neighborhood used by the tabu-search techniques limits channel changes.

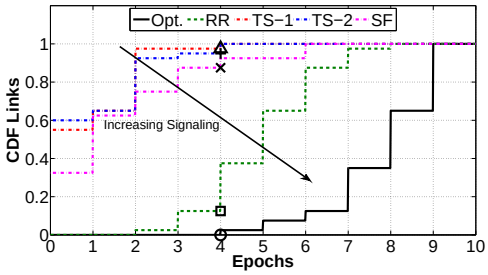

Fig. 7: Channel switching distribution of ZigBee links in a scenario of 40 mobile terminals (5 WBANs for each of the 8 BBNs). The markers represent the percentage of links that switch their channels less than 4 times (i.e., $\mathcal{F}(x < 4)$).

We observe that these new results confirm the trends observed in our previous publication [28]. Therefore, blindly changing ZigBee channels by using a pseudo-random approach, without considering all sources that contribute to CTI, results in a performance loss and higher signaling overhead. This finding is further supported by the results illustrated in the following simulations that compare the performance loss caused by the standard channel hopping approach designed to mitigate CTI for the Bluetooth technology.

From the standpoint of resource utilization, numerical results, which we do not show for the sake of brevity, show that channel switching increases the total number of channels used by the entire system during the simulation. In particular, the solutions provided by TS and LPSF algorithms require all available ZigBee channels to be utilized, without improving significantly the maximum CTI experienced by network nodes. Our results suggest that a good, yet non-perfect, estimation of interfering links permits us to significantly reduce the CTI within the network even when using fixed channels. Therefore, knowledge of interfering transmissions reduces the need for channel switching, since this latter technique achieves similar performance to the one obtained forcing fixed channel assignments despite an increased signaling overhead required to coordinate the devices and an increased use of the available channels.

4) Analysis of the Hysteresis Mechanism: In order to evaluate the overhead caused by the hysteresis threshold, we further implement the iterative version of the sequential fixing algorithm, which computes the channel assignment that minimizes the CTI in each time epoch, and we integrate the hysteresis mechanism to simulate the behavior of the proposed distributed approach. Figure 8 illustrates the system changes (namely the number of times the system must be reconfigured according to the new channel assignment) that we measure in the dynamic network scenario with $T = 20$ epochs varying both the threshold and the number of mobile terminals. Specifically, we consider 2 WiFi and 10 ZigBee channels to limit the number of non-orthogonal frequencies, thus increasing the interference. Furthermore, we vary the hysteresis threshold in the $[1 - 10]\%$ range.

It can be observed that the utilization of the hysteresis mechanism allows to decrease system updates by 75%. Indeed, the gap between the CTI values computed using the old and best channel assignment is larger than the hysteresis threshold only during 5 out of 20 epochs.

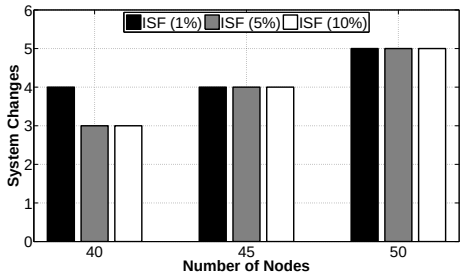

Fig. 8: Number of system changes as a function of the hysteresis threshold and number of nodes (5 Mobile Terminals and for each BBN) in the dynamic scenario with $T = 20$ epochs.

5) Comparison of Channel Switching Techniques: The problem of coexistence of different radio technologies that operate on the same spectrum has been already addressed in the past for devices equipped with both WiFi and Bluetooth radio interfaces. More specifically, three different techniques have been proposed to mitigate the cross-interference between WiFi and Bluetooth technologies on the same device: the *Adaptive Frequency Hopping (AFH)*, *Channel Skipping (CS)*, and *Time Division Multiplexing (TDM)*. Using AFH, a Bluetooth device periodically switches its transmission frequency among a list of low noisy channels, with a switching frequency of 1600 hops per second. The CS technique consists of informing the Bluetooth MAC of the channel used by the WiFi interface to avoid using the same spectrum band of this channel for Bluetooth communications. Finally, the TDM mechanism coordinates the activities of the two radio interfaces to share the same spectrum.

In this work, we evaluate our techniques against those proposed in the Bluetooth standard, implementing both the AFH and CS schemes. Indeed, similar approaches can be easily extended to WBANs based on the ZigBee technology. In particular, we measure the maximum CTI value defined in (4) among the 1600 changes performed by all mobile terminals, applying the AFH and CS techniques to the solution provided by the LPSF algorithm.

Figure 9 illustrates the performance loss caused by the utilization of AFH with CS (AFH + CS) approach with respect to the fixed channel assignment provided by the LPSF algorithm, in the static and dynamic scenarios. In particular, we quantify such performance loss by the "CTI Increment Ratio", defined as $IR = \left[I^{AFH}(t)/I^{SF}(t)\right] - 1$, where $I^{AFH}(t)$ and $I^{SF}(t)$ represent the maximum CTI obtained using AFH and SF, respectively. Figures 9(a) and 9(b) show that AFH+CS increases the CTI independent of nodes mobility, thus reducing the overall quality of the channel assignment computed by the LPSF algorithm. In particular, in the static scenario the measured interference is 40% to 130% higher, whereas in the dynamic scenario the interference increases up to 4 times.

We observe that the performance loss is mainly due to the randomized approach used by the AFH+CS scheme, which skips only the channels used within the same WBAN, without considering the conflicting transmissions of nearby nodes. Indeed, the AFH, CS, and TDM techniques have been proposed for a scenario where the considered interference is only between radio interfaces operating on the same device, which considerably simplifies the CTI mitigation problem. Finally, although the IR decreases with node density, the performance improvement of our solution is still remarkable (up to 1.5x in the dynamic scenario with 50 WBANs).

The comparative results illustrated above confirm the limits of the current approaches to reduce cross-technology interference and the validity of our solution that tackles the problem from the system perspective.

VIII. Conclusion

In this paper, we addressed the Mutual and Cross-Technology Interference mitigation (CTIM) problem in a BBN system, composed of several body-to-body networks. We formulated the interference mitigation problem across different wireless technologies (i.e., ZigBee and WiFi) as an optimization problem, and we introduced a new conflict graph to represent interfering wireless links that use different radio access technologies. To solve efficiently (i.e., in polynomial time) the CTIM problem for large-scale BBN instances, we developed three heuristic approaches based on randomized rounding, tabu-search, and sequential fixing techniques. We further presented a protocol to disseminate the information necessary for constructing the conflict graph and computing the channel assignment that minimizes the CTI in a fully distributed fashion. We evaluated the performance of the proposed algorithms considering both static and dynamic scenarios, illustrating the sensitivity of our algorithms to different parameters, including BBN density, the number of available WiFi channels, the utilization of the channel switching and hysteresis techniques. Numerical results showed that the tabu-search and sequential fixing techniques well approach the optimal solution, yet in polynomial time. In particular, the gap between the LSPF and optimal solution is always lower than 15% and goes to zero when there is only one available WiFi channel.

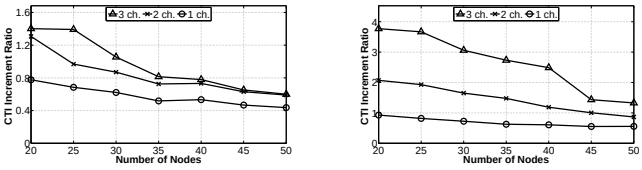

(a) Static scenario (b) Dynamic scenario

Fig. 9: Performance loss caused by the utilization of the Adaptive Frequency Hopping with Channel Skipping (AFH + CS) approach with respect to the sequential fixing (LPSF) algorithm.

Acknowledgement

M. Krunz was supported in part by the National Science Foundation (grant IIP-1265960) and by the Army Research Office (grant W911NF-13-1-0302). Any opinions, findings, conclusions, or recommendations expressed in this paper are those of the author(s) and do not necessarily reflect the views of NSF or ARO.

References

[1] "Google Project Glass." *Available on-line at https://plus.google.com/+projectglass*.

[2] C. Liang, N. Priyantha, J. Liu, and A. Terzis, "Surviving Wi-Fi Interference in Low Power Zigbee Networks," *ACM SenSys*, pp. 309–322, 2010.

[3] G. Santagati, T. Melodia, L. Galluccio, and S. Palazzo, "Ultrasonic Networking for E-health Applications," *IEEE Wireless Commun.*, vol. 20, no. 4, 2013.

[4] M. Kavehrad, "Sustainable Energy-Efficient Wireless Applications Using Light," *IEEE Communications Magazine*, vol. 48, no. 12, pp. 66–73, 2010.

[5] J. Hou, B. Chang, D. Cho, and M. Gerla, "Minimizing 802.11 Interference on ZigBee Medical Sensors," *ICST BODYNETS*, 2009.

[6] J. Huang, G. Xing, G. Zhou, and R. Zhou, "Beyond Co-existence: Exploiting WiFi White Space for Zigbee Performance Assurance," *IEEE ICNP*, pp. 305–314, 2010.

[7] K. Srinivasan, M. Kazandjieva, S. Agarwal, and P. Levis, "The β-factor: Measuring Wireless Link Burstiness," *ACM SenSys*, pp. 29–42, 2008.

[8] K. Srinivasan, M. Jain, J. Choi, T. Azim, E. Kim, P. Levis, and B. Krishnamachari, "The κ factor: Inferring Protocol Performance Using Inter-link Reception Correlation," *ACM MobiCom*, 2010.
[9] X. Zhang and K. Shin, "Enabling Coexistence of Heterogeneous Wireless Systems: case for ZigBee and WiFi," *ACM MobiHoc*, 2011.
[10] ——, "Cooperative Carrier Signaling: Harmonizing Coexisting WPAN and WLAN Devices," *IEEE/ACM Trans. on Networking*, vol. 21, no. 2, pp. 426–439, 2013.
[11] K. Lakshminarayanan, S. Seshan, and P. Steenkiste, "Understanding 802.11 Performance in Heterogeneous Environments," *ACM SIGCOMM HomeNets*, pp. 43–48, 2011.
[12] A. Subramanian, H. Gupta, S. Das, and J. Cao, "Minimum Interference Channel Assignment in Multiradio Wireless Mesh Networks," *IEEE Trans. on Mobile Computing*, vol. 7, no. 12, pp. 1459–1473, 2008.
[13] S. Cheng and C. Huang, "Coloring-Based Inter-WBAN Scheduling for Mobile Wireless Body Area Networks," *IEEE Trans. on Parallel and Distributed Systems*, vol. 24, no. 2, pp. 250–259, 2013.
[14] Q. Wang, D. Wu, and P. Fan, "Delay-Constrained Optimal Link Scheduling in Wireless Sensor Networks," *IEEE Trans. on Vehicular Technology*, vol. 59, no. 9, pp. 4564–4577, 2010.
[15] A. Mishra, V. Shrivastava, S. Banerjee, and W. Arbaugh, "Partially Overlapped Channels not Considered Harmful," *ACM SIGMETRICS Performance Evaluation Review*, vol. 34, no. 1, pp. 63–74, 2006.
[16] P. Costa, C. Mascolo, M. Musolesi, and G. Picco, "Socially-Aware Routing for Publish-Subscribe in Delay-Tolerant Mobile Ad Hoc Networks," *IEEE J. Select. Areas Commun.*, vol. 26, no. 5, pp. 748–760, 2008.
[17] J. Padhye, S. Agarwal, V. Padmanabhan, L. Qiu, A. Rao, and B. Zill, "Estimation of Link Interference in Static Multi-Hop Wireless Networks," *The 5th ACM SIGCOMM Conference on Internet Measurement*, 2005.
[18] A. Raniwala, K. Gopalan, and T. Chiueh, "Centralized Channel Assignment and Routing Algorithms for Multi-Channel Wireless Mesh Networks," *ACM SIGMOBILE Mobile Computing and Communications Review*, vol. 8, no. 2, pp. 50–65, 2004.
[19] F. Glover, "Tabu search. part i and ii," *ORSA Journal on Computing*, vol. 1, pp. 190–206, 1989/90.
[20] T. Shu and M. Krunz, "Exploiting Microscopic Spectrum Opportunities in Cognitive Radio Networks via Coordinated Channel Access," *IEEE Trans. on Mobile Computing*, vol. 9, no. 11, pp. 1522–1534, 2010.
[21] H. Salameh, M. Krunz, and D. Manzi, "Spectrum Bonding and Aggregation with Guard-band Awareness in Cognitive Radio Networks," *IEEE Trans. on Mobile Computing*, vol. 13, no. 3, pp. 569–581, 2013.
[22] N. Theis, R. Thomas, and L. DaSilva, "Rendezvous for Cognitive Radios," *IEEE Trans. on Mobile Computing*, vol. 10, no. 2, pp. 216–227, 2011.
[23] Y. Song and J. Xie, "A Distributed Broadcast Protocol in Multi-hop Cognitive Radio Ad hoc Networks Without a Common Control Channel," *IEEE INFOCOM*, pp. 2273–2281, 2012.
[24] M. Abdel-Rahman, S. Phillips, R. Sanfelice, and M. Krunz, "Adaptive Frequency Hopping and Synchronization-Based Algorithms for Rendezvous," *IEEE DySPAN*, pp. 517–528, 2012.
[25] E. A. Tobagi and L. Kleinrock, "Packet Switching in Radio Channels: Part II – The Hidden Terminal Problem in Carrier Sense Multiple Access Modes and the Busy-tone Solution," *IEEE Trans. on Communications*, vol. 23, no. 12, pp. 1417–1433, 1975.
[26] M. Abolhasan, T. Wysocki, and E. Dutkiewicz, "A Review of Routing Protocols for Mobile Ad hoc Networks," *Ad Hoc Networks*, vol. 2, no. 1, pp. 1–22, 2004.
[27] G. Pei, M. Gerla, and T.-W.Chen, "Fisheye State Routing: A Routing Scheme for Ad hoc Wireless Networks," *IEEE ICC*, pp. 70–74, 2000.
[28] S. Paris, J. Elias, and A. Mehaoua, "Cross Technology Interference Mitigation in Body-to-Body Area Networks," *IEEE WoWMoM*, pp. 1–9, Madrid, Spain, June 2013.
[29] M. Cheng, X. Gong, L. Cai, and X. Jia, "Cross-Layer Throughput Optimization With Power Control in Sensor Networks," *IEEE Trans. on Vehicular Technology*, vol. 60, no. 7, pp. 3300–3308, 2011.
[30] D. Johnson and D. Maltz, "Dynamic Source Routing in Ad-Hoc Wireless Networks," *Mobile computing*, vol. 353, pp. 153–181, 1996.

Jocelyne Elias is Associate Professor at Paris Descartes University since September 2010. She obtained her Ph.D. in Information and Communication Technology at the Department of Electronics and Information of Politecnico di Milano in 2009. Her main research interests include network optimization, and in particular modeling and performance evaluation of networks (Cognitive Radio, Wireless, Overlay and Wired Networks), as well as the application of Game Theory to resource allocation, spectrum access, and pricing problems.

Stefano Paris is an Assistant Professor at LIPADE (Laboratoire d'Informatique Paris Descartes), the department of Computer Science at Paris Descartes University. He received his M.S. degree in Computer Engineering from University of Bergamo in 2007, and the Ph.D. in Information Engineering from Politecnico di Milano in 2011. His main research interests include protocol design and performance evaluation of wireless networks, security, network design and optimization.

Marwan Krunz is a professor of ECE and CS at the University of Arizona. He is the site co-director of the Broadband Wireless Access and Applications Center, a NSF/industry IUCRC center that includes five universities and 20+ industry members. From 2008-2014, he was the site director of the NSF IUCRC "Connection One" center. Dr. Krunz received his Ph.D. degree in electrical engineering from Michigan State University in 1995. He joined the University of Arizona in January 1997, after a brief postdoctoral stint at the University of Maryland. In 2010, he was a Visiting Chair of Excellence at the University of Carlos III de Madrid, and concurrently a visiting researcher at Institute IMDEA Networks. In 2011, he received a Fulbright Senior Expert award, through which he visited with the University of Jordan, King Abdullah II School of Information Technology. He previously held other visiting research positions at INRIA-Sophia Antipolis, HP Labs, University of Paris VI, University of Paris V, and US West Advanced Technologies. Dr. Krunz's research interests lie in the areas of wireless communications and networking, with emphasis on resource management, adaptive protocols, and security issues. Recently, he has been involved in projects related to dynamic spectrum access, wireless security, power-controlled protocols for wireless networks, multi-channel MIMO systems, secure satellite communications, energy management in solar-powered WSNs, and full-duplex communications. He has published more than 220 journal articles and peer-reviewed conference papers, and is a co-inventor on five US patents. M. Krunz is an IEEE Fellow, an Arizona Engineering Faculty Fellow (2011-2014), and an IEEE Communications Society Distinguished Lecturer (2013 and 2014). He was the recipient of the 2012 IEEE Communications Society's TCCC Outstanding Service Award. He received the NSF CAREER award in 1998. He currently serves on the editorial board for the IEEE Transactions on Network and Service Management. Previously, he served on the editorial boards for the IEEE/ACM Transactions on Networking, the IEEE Transactions on Mobile Computing, the Computer Communications Journal, and the IEEE Communications Interactive Magazine. He was a guest co-editor for special issues in IEEE Micro and IEEE Communications Magazines. He was the general co-chair for the ACM WiSec 2012 Conference, and served as a TPC chair for various international conferences, including INFOCOM'04, SECON'05, and WoWMoM'06. He has served and continues to serve on the executive and technical program committees of numerous international conferences, and on the panels of several funding agencies. He was the keynote speaker, an invited panelist, and a tutorial presenter at various international conferences.